Blind Doppler Tracking and Positioning with NOAA LEO Satellite Signals

Sharbel Kozhaya, Haitham Kanj, and Zaher M. Kassas
The Ohio State University

BIOGRAPHY

Sharbel Kozhaya is a Ph.D student in the Department of Electrical and Computer Engineering at The Ohio State University and a member of the Autonomous Systems Perception, Intelligence, and Navigation (ASPIN) Laboratory. He received a B.E. in Electrical Engineering from the Lebanese American University. His current research interests include opportunistic navigation, low Earth orbit (LEO) satellites, cognitive software-defined radio, and 5G. He is the recipient of the 2023 IEEE/ION Position, Location, and Navigation Symposium (PLANS) best student paper award.

Haitham Kanj is a Ph.D student in the Department of Electrical and Computer Engineering at The Ohio State University and a member of the Autonomous Systems Perception, Intelligence, and Navigation (ASPIN) Laboratory. He received a B.E. in Electrical Engineering from the Lebanese American University. His current research interests include opportunistic navigation, low Earth orbit (LEO) satellites, and cognitive software-defined radio. He is the recipient of the 2023 IEEE/ION Position, Location, and Navigation Symposium (PLANS) best student paper award.

Zaher (Zak) M. Kassas is a professor at The Ohio State University and TRC Endowed Chair in Intelligent Transportation Systems. He is the Director of the Autonomous Systems Perception, Intelligence, and Navigation (ASPIN) Laboratory. He is also director of the U.S. Department of Transportation Center: CARMEN (Center for Automated Vehicle Research with Multimodal AssurEd Navigation), focusing on navigation resiliency and security of highly automated transportation systems. He received a B.E. in Electrical Engineering from the Lebanese American University, an M.S. in Electrical and Computer Engineering from The Ohio State University, and an M.S.E. in Aerospace Engineering and a Ph.D. in Electrical and Computer Engineering from The University of Texas at Austin. He is a recipient of the National Science Foundation (NSF) CAREER award, Office of Naval Research (ONR) Young Investigator Program (YIP) award, Air Force Office of Scientific Research (AFOSR) YIP award, IEEE Walter Fried Award, Institute of Navigation (ION) Samuel Burka Award, and ION Col. Thomas Thurlow Award. He is an Associate Editor of the IEEE Transactions on Aerospace and Electronic Systems and the IEEE Transactions on Intelligent Transportation Systems. He is a Fellow of the ION and a Distinguished Lecturer of the IEEE Aerospace and Electronic Systems Society. His research interests include cyber-physical systems, navigation systems, and intelligent transportation systems.

ABSTRACT

A spectral approach for blind acquisition and Doppler tracking of low Earth orbit (LEO) satellite signals is applied to National Oceanic and Atmospheric Administration (NOAA) satellites. The approach accounts for the high LEO satellites' dynamic channel, by deriving an appropriate model for the received signal frequency spectrum. A frequency-domain-based Doppler discriminator is utilized along with a Kalman filter-based Doppler tracking algorithm. Experimental results are presented showing successful acquisition and Doppler tracking of NOAA LEO satellite signals. Next, the approach is demonstrated in multi-constellation LEO acquisition and tracking, showing Hz-level Doppler tracking of 4 Starlink, 2 OneWeb, 1 Iridium NEXT, 1 Orbcomm, and 1 NOAA LEO satellites. Carrier phase observables were constructed from the tracked Doppler and fused through a nonlinear least-squares estimator to localize a stationary receiver. Starting with an initial estimate 3,600 km away from the receiver's true position, the proposed approach is shown to achieve a two-dimensional (2D) error of 5.1 m.

I. INTRODUCTION

Navigation from low Earth orbit (LEO) satellites promises to revolutionize satellite-based navigation (Kassas et al., 2019; Jardak and Jault, 2022; Prol et al., 2022; Janssen et al., 2023; Menzione and Paonni, 2023; Prol et al., 2023). As such, it is not surprising to witness the tremendous interest from governments and private technology giants, launching their own LEO constellations, some of which dubbed "megaconstellations" as they will comprise thousands of LEO satellites (Curzi et al., 2020; Liu et al., 2021).

Using LEO satellite signals for navigation offers several desirable attributes (Reid et al., 2021; Kassas, 2021): (i) higher received signal power compared to GNSS satellites that reside in medium Earth orbit (MEO), (ii) high availability and favorable geometry, and (iii) spectral diversity in the radio frequency spectrum. However, exploiting broadband LEO satellite signals of opportunity

Preprint of the 2023 ION GNSS+ Conference
Denver, Colorado, September 11–15, 2023

for navigation purposes comes with challenges, as they are owned by private operators that typically do not disclose crucial information about the satellites': (i) ephemerides, (ii) clock synchronization and stability, and (iii) signal specifications.

Several studies have been published over the past few years addressing the aforementioned challenges, from addressing satellite orbit, clock, and propagation errors (Mortlock and Kassas, 2021; Khairallah and Kassas, 2021; Morton et al., 2022; Cassel et al., 2022; Wang et al., 2023; Zhao et al., 2023; Wu et al., 2023; Jiang et al., 2023; Ye et al., 2023; Khalife and Kassas, 2023; Saroufim et al., 2023; Kassas et al., 2023a); to receiver and signal design (Tan et al., 2019; Wei et al., 2020; Bilardi, 2021; Orabi et al., 2021; Kassas et al., 2021; Neinavaie et al., 2022b; Egea-Roca et al., 2022; Huang et al., 2022; Pinell et al., 2023; Yang et al., 2023; Humphreys et al., 2023; Yang and Soloviev, 2023); to analyzing the estimation performance (Farhangian et al., 2021; Psiaki, 2021; Hartnett, 2022; Singh et al., 2022; Jiang et al., 2022; More et al., 2022; Shi et al., 2023; Guo et al., 2023; Kanamori et al., 2023; Sabbagh and Kassas, 2023; Farhangian and Landry, 2023; Ries et al., 2023).

This paper focuses on addressing the challenge of extracting navigation observables from unknown LEO satellite signals. Whenever the LEO downlink signal structure is sufficiently known, designing a receiver that could acquire and track such signals becomes a "classic" receiver design problem. Examples of LEO constellations with sufficient knowledge about their downlink signal include Orbcomm and Iridium NEXT. Nevertheless, new LEO megaconstellations, such as Starlink and OneWeb, do not disclose public information about their signals. This challenge can be addressed with blind signal processing techniques. Previous research was capable of estimating downlink sequences in direct sequence spread spectrum communication systems (Tsatsanis and Giannakis, 1997; Burel and Bouder, 2000; Choi and Moon, 2020; Li et al., 2023), for GPS/GNSS signals under non-cooperative conditions (Merwe et al., 2020; Rui et al., 2022), and for orthogonal frequency-division multiplexing (OFDM) signals (Bolcskei, 2001; Tanda, 2004; Liu et al., 2010). However, LEO downlink channels pose a challenge making the aforementioned approaches not straightforwardly applicable, namely the high dynamics of the channel between the LEO satellite and the ground-based receiver. To address this challenge in the context of LEO, (Neinavaie et al., 2021; Kozhaya and Kassas, 2022) developed blind Doppler tracking approaches that were used to navigate an unmanned aerial vehicle (UAV) with Obrcomm LEO satellites; while (Khalife et al., 2022) was the first to successfully apply blind signal processing techniques on Starlink LEO signals, yielding carrier phase observables, from which a stationary receiver was localized with a two-dimensional (2D) error of 25.9 m with signals from six Starlink LEO satellites. Another blind approach, based on matched subspace detection, was developed in (Neinavaie et al., 2022a; Neinavaie and Kassas, 2023), yielding Doppler observables, from which a stationary receiver was localized with a 2D error of 10 m (with pure tones) and 6.5 m (with OFDM signals in addition to pure tones) from the same six Starlink LEO satellites. A blind spectral-based approach was developed in (Kozhaya and Kassas, 2023), yielding Doppler observables, from which a stationary receiver was localized with a 2D error of 4.3 m with the same six Starlink LEO satellites. In (Kozhaya et al., 2023; Kassas et al., 2023b), it was demonstrated that this approach is rather general, referred to as LEO-agnostic, and is capable of acquiring and tracking LEO signals regardless of their modulation and multiple access schemes. In addition to Starlink LEO, the approach was successfully applied to OneWeb, Orbcomm, and Iridium NEXT LEO satellites, yielding Hz-level-accurate Doppler tracking, from which a stationary receiver was localized with a 2D error of 5.1 m with 2 OneWeb, 4 Starlink, 1 Iridium NEXT, and 1 Orbcomm LEO satellites. This paper shows that this LEO-agnostic approach is capable of exploiting the signals of a fifth LEO constellation: National Oceanic and Atmospheric Administration (NOAA) satellites.

This paper offers the following contributions: (i) derive an analytical approximation of the received signal frequency spectrum for highly dynamic channels and (ii) develop a blind Doppler spectral estimator via frequency-domain cross-correlation and a Kalman filter (KF)-based tracking loop. The proposed approach relies on the presence of a repetitive sequence in the LEO satellite's downlink, to which the blind spectral Doppler tracker locks and cross-correlation is used to track the Doppler shift. Experimental results are presented showing successful acquisition and Doppler tracking of NOAA LEO satellite signals with the proposed approach. In addition, experimental results are presented showing Hz-level Doppler tracking of 4 Starlink, 2 OneWeb, 1 Iridium NEXT, 1 Orbcomm, and 1 NOAA LEO satellites. Carrier phase observables are constructed from the tracked Doppler and fused through a nonlinear least-squares (NLS) estimator to localize a stationary receiver. Starting with an initial estimate 3,600 km away from the receiver's true position, the proposed approach is shown to achieve a two-dimensional (2D) error of 5.1 m.

This paper is organized as follows. Section II derives the signal model. Section III discusses the blind Doppler discriminator and tracking approach. Section IV presents NOAA LEO tracking results. Section V presents multi-constellation LEO tracking and positioning with Starlink, OneWeb, Iridium NEXT, Orbcomm, and NOAA LEO satellites. Section VI gives concluding remarks.

II. SIGNAL MODEL

This section presents a model of the received signal, which takes into account the high dynamics channel between the LEO satellite and ground-based receiver. Then, it derives an analytical expression of the signal's frequency spectrum.

1. Received Baseband Signal Model

Let $x(t)$ be the unknown LEO satellite signal, expressed at baseband. The proposed framework does not assume any particular modulation or multiplexing scheme. The only assumption is that $x(t)$ can be written as $x(t) = s(t) + n_d(t)$, where $s(t)$ is a deterministic repetitive signal and $n_d(t)$ is a random signal driven by the user data. Examples of repetitive sequences are the pseudorandom noise (PRN) used in GPS (Flores (2022)), Globalstar LEO satellites (Hendrickson (1997)), and CDMA2000 (3GPP2 (2011)) and the primary and secondary synchronization sequences (PSS and SSS) used in 4G long-term evolution (LTE) (3GPP (2010)) and 5G (3GPP (2018)). The proposed framework assumes the following properties of $s(t)$:

1. It is periodic with period T_0.
2. It is uncorrelated with the data $n_d(t)$.
3. It is zero-mean, has a stationary power spectral density (PSD) with $\left|\mathcal{F}\left\{s(t)w_{T_0}(t)\right\}\right|^2 = S_s(f)$, where $w_{T_0}(t)$ is a windowing function that is unity within the interval $[0, T_0]$ and zero elsewhere.

Consider $x(t)$ being transmitted at a carrier frequency f_c. Let $\tau_d(t)$ denote the apparent delay between the transmitted signal $x_c(t) \triangleq x(t)\exp(j2\pi f_c t)$ and the received signal at the receiver's antenna. The apparent delay $\tau_d(t)$ is composed of (i) the time-of-flight along the line-of-sight (LOS) between the transmitter and receiver (i.e., $d_{LOS}(t)/c$, where $d_{LOS}(t)$ is the LOS distance between the LEO satellite's transmitter and the receiver and c is the speed of light); (ii) combined effect of the transmitter's and receiver's clock biases, denoted $\delta t_{clk}(t)$; (iii) ionospheric and tropospheric delays $\delta t_{iono}(t)$ and $\delta t_{tropo}(t)$, respectively; and (iv) other unmodeled errors. After propagating in an additive white Gaussian channel, the resulting received signal before baseband mixing can be expressed as

$$\bar{r}(t) = x_c\left(t - \tau_d(t)\right) + \bar{n}(t) = x(t - \tau_d(t))\exp\left(j2\pi f_c\left[t - \tau_d\left(t\right)\right]\right) + \bar{n}(t),$$

where $\bar{n}(t)$ is a complex white Gaussian noise with PSD $N_0/2$.

Let $r(t) \triangleq \bar{r}(t)\exp\left(-j2\pi f_c t\right)$ denote the received signal after baseband mixing and filtering. Then, $r(t)$ can be expressed as $r(t) = x(t - \tau_d(t))\exp\left(j\theta(t)\right) + n(t)$, where $n(t)$ is the low-pass filter output of $\bar{n}(t)$, and $\theta(t) = -2\pi f_c \tau_d(t)$ is the carrier phase of the received signal. Using a Taylor series expansion, at time instant $t_k = t_0 + kT_0$, where k is the sub-accumulation index and t_0 is some initial time, the carrier phase of the signal can be expressed as

$$\theta(t) = \theta(t_k) + \dot{\theta}(t_k)t + \frac{1}{2}\ddot{\theta}(t_k)t^2 + H.O.T. \tag{1}$$

Denote $\theta_k(t)$ as $\theta(t)$ in (1), after dropping the higher-order terms ($H.O.T.$). By definition, $f_D(t) \triangleq \frac{\dot{\theta}(t)}{2\pi}$ is the apparent Doppler shift and $\dot{f}_D(t)$ is the apparent Doppler rate.

It is important to note that the channel between the LEO satellite and the ground-based receiver is highly dynamic, thus, high Doppler shift and rate will be observed by the receiver. On the other hand, at the k-th sub-accumulation, $\tau_d(t)$ is approximated by its zero-order term $d_k = \tau_d(t_k)$, while the higher order terms are dropped to simplify the following signal analysis. Due to the first property, one can arbitrarily choose $\tau_d(t)$ to denote the code start time. It is important to note that the higher order terms in $\tau_d(t)$ stretch or contract the code in the time-domain, but this paper ignores this effect, which seems to be of little impact on Starlink LEO satellite codes.

Finally, the expression of the received signal at the k-th sub-accumulation can be written as $r_k^-(t) = r(t)w_{T_0}(t - t_k) = s_k(t)\exp\left(j\theta_k(t)\right) + n_k^-(t)$, where $s_k(t) = s(t - d_k)w_{T_0}(t)$ and $n_k^-(t) = n(t - d_k)w_{T_0}(t)$. The received signal $r_k(t)$ after carrier wipe-off using the carrier phase estimate, denoted $\hat{\theta}_k(t)$, generated by the tracking loop discussed in Section III.2, can be expressed as

$$r_k(t) = r_k^-(t)\exp(-j\hat{\theta}_k(t)) = s_k(t)\exp(j\tilde{\theta}_k(t)) + n_k(t), \tag{2}$$

where $\tilde{\theta}_k(t) = \theta_k(t) - \hat{\theta}_k(t)$ is the residual carrier phase.

2. Frequency Spectrum of the Received Signal

The received signal's frequency spectrum at the k-th sub-accumulation is $S_{r_k}(f) = |\mathcal{F}\{r_k(t)\}|^2$. Using the third property of $s(t)$, the Wigner distribution function (WDF) of $s_k(t)$ for $t \in [0, T_0]$ can be written as

$$W_s(t,f) \triangleq \int_{-\infty}^{\infty} s_k\left(t+\frac{\tau}{2}\right) s_k^*\left(t-\frac{\tau}{2}\right) \exp(-2\pi f\tau)\, d\tau = \frac{S_s(f)}{T_0}.$$

It can be shown that the WDF of the residual carrier phase at the k-th sub-accumulation $C_k(t) = \exp(j\tilde{\theta}_k(t))$, for $t \in [0, T_0]$, is $W_{C_k}(t,f) = \delta\left(f - \frac{\dot{\tilde{\theta}}_k}{2\pi} - \frac{\ddot{\tilde{\theta}}_k}{2\pi}t\right)$, where $\delta(\cdot)$ denotes the Dirac delta function. Using the second property of $s(t)$, the WDF of $r_k(t)$ in (2), for $t \in [0, T_0]$, can be written as

$$W_{r_k}(t,f) = \frac{S_s(f)}{T_0} \circledast \delta\left(f - \frac{\dot{\tilde{\theta}}_k}{2\pi} - \frac{\ddot{\tilde{\theta}}_k}{2\pi}t\right) + W_{n_k}(t,f),$$

where $(f \circledast g)(t) = \int_{-\infty}^{\infty} f(\tau)g(t-\tau)d\tau$ is the convolution, $W_{n_k}(t,f)$ is the WDF of the noise and data at the k-th sub-accumulation. Using the projection property of WDF, the following follows

$$\begin{aligned} S_{r_k}(f) &\triangleq \int_0^{T_0} W_{r_k}(t,f)\, dt = \frac{S_s(f)}{T_0} \circledast \int_0^{T_0} \delta\left(f - \frac{\dot{\tilde{\theta}}_k}{2\pi} - \frac{\ddot{\tilde{\theta}}_k}{2\pi}t\right) dt + S_{n_k}(f) \\ &= S_s(f) \circledast \frac{2\pi}{\left|\ddot{\tilde{\theta}}_k\right| T_0} \int_0^{T_0} \delta\left(t - \frac{2\pi f - \dot{\tilde{\theta}}_k}{\ddot{\tilde{\theta}}_k}\right) dt + S_{n_k}(f) = S_s(f) \circledast \Pi\left(f; \dot{\tilde{\theta}}_k, \ddot{\tilde{\theta}}_k\right) + S_{n_k}(f), \end{aligned} \tag{3}$$

where $S_{n_k}(f) = \int_0^{T_0} W_{n_k}(t,f)\, dt$ and

$$\Pi\left(f; \dot{\theta}, \ddot{\theta}\right) = \frac{2\pi}{\left|\ddot{\theta}\right| T_0} \begin{cases} 1, & \left| f - \dfrac{\dot{\theta} + \dfrac{|\ddot{\theta}|}{2} T_0}{2\pi} \right| < \dfrac{|\ddot{\theta}|}{4\pi} T_0, \\ 0, & \text{elsewhere.} \end{cases}$$

Equation (3) states that the received signal's frequency spectrum consists of a shifted and dilated version of the repetitive sequence's frequency spectrum alongside a noise floor. The shifting in the received spectrum is mainly due to residual Doppler $\dot{\tilde{\theta}}_k$ and the dilation is due to residual Doppler rate $\ddot{\tilde{\theta}}_k$.

III. BLIND DOPPLER TRACKING

This section derives the Doppler discriminator and formulates the KF-based Doppler tracking loop.

1. Frequency-Domain Based Doppler Discriminator

The nonlinear NLS estimator of the residual Doppler $\dot{\tilde{\theta}}_k$ at the k-th sub-accumulation is given by

$$\begin{aligned} \dot{\tilde{\theta}}_k &= \underset{\dot{\theta}}{\operatorname{argmin}} \left\| S_{r_k}(f) - S_s(f) \circledast \Pi\left(f; \dot{\theta}, \ddot{\theta}\right) \right\|^2 \\ &= \underset{\dot{\theta}}{\operatorname{argmin}} \left\| S_{r_k}(f) \right\|^2 + \left\| S_s(f) \circledast \Pi\left(f; \dot{\theta}, \ddot{\theta}\right) \right\|^2 - 2\left(S_{r_k} \star S_s\right)(f) \circledast \Pi\left(f; \dot{\theta}, \ddot{\theta}\right) \qquad (4) \\ &= \underset{\dot{\theta}}{\operatorname{argmax}} \left(S_{r_k} \star S_s\right)(f) \circledast \Pi\left(f; \dot{\theta}, \ddot{\theta}\right) \cong \underset{\dot{\theta}}{\operatorname{argmax}} \left(S_{r_k} \star S_s\right)(f) \circledast \delta\left(f - \frac{\dot{\theta}}{2\pi}\right), \quad \text{for} \quad \ddot{\tilde{\theta}}_k \approx 0 \\ &= 2\pi \underset{f}{\operatorname{argmax}} \left(S_{r_k} \star S_s\right)(f), \qquad (5) \end{aligned}$$

where $(f \star g)(\tau) = \int_{-\infty}^{\infty} f^*(t)g(t+\tau)dt$ is the cross-correlation. The first two terms in the minimization problem (4) are a constant function of the search parameter $\dot{\theta}$; therefore, they are ignored. As the blind receiver does not have prior knowledge of $S_s(f)$, it starts with an initial estimate $\hat{S}_s(f) \triangleq S_{r_0}(f)$ and refines the repetitive sequence's spectrum with every sub-accumulation. It is worth pointing that the regime of small residual Doppler rate values assumed in (5) is a reasonable assumption, since the Doppler rate between two consecutive sub-accumulations is nearly constant.

2. Kalman Filter-Based Tracking Loop

The continuous-time signal in (2) is sampled at a sampling interval $T_s = 1/F_s$, the discrete-time received signal before carrier wipe-off at the k-th sub-accumulation can be written as

$$r_k^-[n] = s[n - d_k] \exp\left(j\tilde{\Theta}_k[n]\right) + n_k^-[n],$$

where $n \in [0, L-1]$, $s[n]$ is the discrete-time sequence of $s(t)$ with period $L = T_0/T_s$ and $\tilde{\Theta}_k[n]$ and d_k are the discrete-time carrier phase and code start time, respectively, of the received signal at the k-th sub-accumulation.

The carrier phase state vector is defined as $\boldsymbol{\theta}(t) \triangleq \left[\theta(t),\ \dot{\theta}(t),\ \ddot{\theta}(t)\right]^{\mathsf{T}}$, whose dynamics is modeled as

$$\dot{\boldsymbol{\theta}}(t) = \mathbf{A}\boldsymbol{\theta}(t) + \mathbf{B}\boldsymbol{w}(t), \tag{6}$$

$$\mathbf{A} \triangleq \begin{bmatrix} 0 & 1 & 0 \\ 0 & 0 & 1 \\ 0 & 0 & 0 \end{bmatrix}, \quad \mathbf{B} \triangleq \begin{bmatrix} 0 \\ 0 \\ 1 \end{bmatrix},$$

where $\boldsymbol{w}(t)$ is a zero-mean white noise process with power spectral density q_w. The continuous-time dynamics in (6) is discretized at a sampling time $T_0 = LT_s$, leading to $\boldsymbol{\Theta}_{k+1} = \mathbf{F}\boldsymbol{\Theta}_k + \mathbf{w}_k$, where $\boldsymbol{\Theta}_k \triangleq \left[\theta_k,\ \dot{\theta}_k,\ \ddot{\theta}_k\right]^{\mathsf{T}}$, $\mathbf{F} \triangleq e^{\mathbf{A}T_0}$ is the state transition matrix, $\mathbf{w}_k$ is a discrete-time process noise vector, which is a zero-mean white sequence with covariance $\mathbf{Q} = q_{\tilde{w}} \int_0^{T_0} e^{\mathbf{A}t}\mathbf{B}\left(e^{\mathbf{A}t}\mathbf{B}\right)^{\mathsf{T}} dt$. The reconstructed sequence of the carrier phase used to perform carrier wipe-off can be written as a second order piece-wise polynomial given by $\hat{\Theta}_k[n] = \hat{\theta}_{k-1} + \hat{\dot{\theta}}_k nT_s + \frac{1}{2}\hat{\ddot{\theta}}_k (nT_s)^2$, $n \in [0, L-1]$. After carrier wipe-off, the received signal's sequence can be expressed as

$$r_k[n] = s[n - d_k] \exp\left(j\tilde{\Theta}_k[n]\right) + n_k[n]. \tag{7}$$

Equation (7) will be used to determine the residual Doppler $\tilde{\dot{\theta}}_k$ at the k-th sub-accumulation, which is fed as innovation to a KF loop that uses the observation model $z_k = \mathbf{H}\boldsymbol{\Theta}_k + v_k$, where $\mathbf{H} \triangleq [0\ 1\ 0]$ and v_k is a discrete-time zero-mean white noise sequence with variance $\sigma_{\dot{\theta}}^2$. The KF innovation ν_k is the fast Fourier transform (FFT)-based discrete-time version of (5).

$$\nu_k = \tilde{\dot{\theta}}_k = \underset{\dot{\theta}}{\operatorname{argmax}} \left|R_k[\dot{\theta}]\right|^2 \star \left|\hat{S}_k[\dot{\theta}]\right|^2.$$

It is worth noting that the Doppler tracked using the proposed approach has a real-valued ambiguity part $\dot{\theta}_N$ that needs to be resolved to retrieve back the actual Doppler shift.

IV. EXPERIMENTAL RESULTS: NOAA LEO ACQUISITION AND TRACKING

This section demonstrates the proposed blind Doppler estimator and tracking loop with NOAA LEO satellite signals. To this end, a stationary National Instrument (NI) universal software radio peripheral (USRP) E312 was equipped with a consumer-grade very high frequency (VHF) Quadrifilar Helical antenna to receive NOAA LEO satellite signals. The sampling bandwidth was set to 2.4 MHz and the carrier frequency f_c was set to 137.0 MHz. Samples of the VHF signal were stored for off-line processing via a software-defined radio (SDR).

The USRP was set to record for a period of 800 seconds. During this period, one NOAA satellite passed over the receiver. The framework discussed in Section III was used to acquire and track the signal from the satellite with $q_w = (0.1)^2$ rad^2/s^6 and $\sigma_{\dot{\theta}} = \frac{\pi}{6}$ rad/s. The estimated beacon spectrum and tracked Doppler from the satellite is shown in Figure 1.

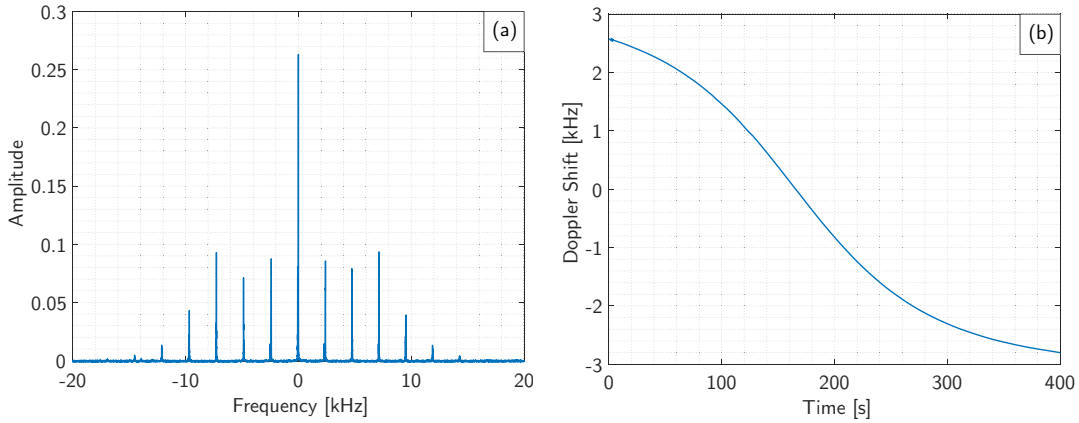

Figure 1: (a) NOAA LEO satellite estimated beacon spectrum. (b) Blindly tracked Doppler from a NOAA satellite using the spectral-based approach.

V. EXPERIMENTAL RESULTS: STARLINK, ONEWEB, ORBCOMM, IRIDIUM NEXT, AND NOAA LEO TRACKING AND POSITIONING

This section presents multi-constellation tracking and positioning results, exploiting signals from Starlink, OneWeb, Orbcomm, Iridium NEXT, and NOAA LEO constellations. The hardware used for data collection (see Figure 2) included: (i) an LNB with conversion gain of 50 dB and noise figure of 2.5 dB connected to a Ku-band 60 cm parabolic offset dish with gain of 30 dBi to receive Starlink and OneWeb satellite signals, (ii) a commercial Orbcomm antenna to receive Orbcomm and NOAA signals, and (iii) a commercial Iridium NEXT antenna.

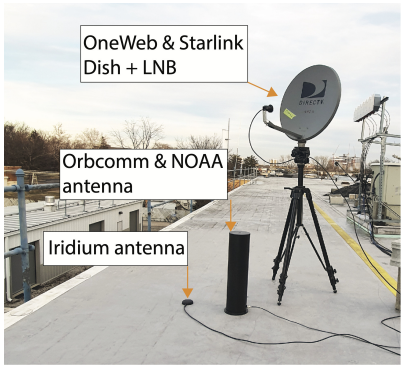

Figure 2: Hardware setup.

Figure 3 shows the tracked Doppler and Doppler error from multi-constellation LEO satellites (4 Starlink, 2 OneWeb, 1 Orbcomm, 1 Iridium NEXT, and 1 NOAA) as well as their respective trajectories during their passing overhead.

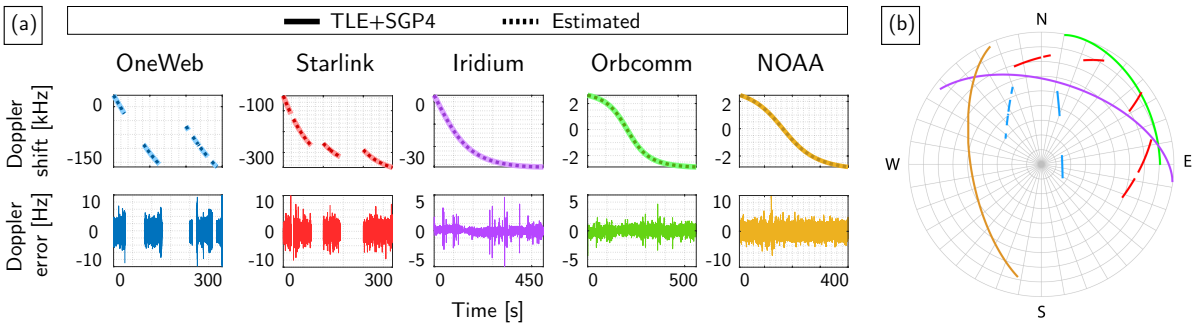

Figure 3: (a) Top: Doppler curves generated by the proposed framework (dashed) and calculated from propagated satellite orbit using TLE+SGP4 (solid). Bottom: the innovation of the KF tracking loops. (b) Skyplot showing the trajectories of the tracked LEO satellites.

After tracking, carrier phase measurements were reconstructed by integrating the tracked Doppler and fed to a batch NLS estimator to estimate the position of the stationary receiver. The measurement model and positioning filter formulation were adopted from (Kozhaya et al., 2023). The receiver's initial position estimate was set on the roof of the Engineering parking structure at the University of California, Irvine, USA, approximately 3,600 km away from the true position, which was on the roof of the ElectroScience Laboratory at the The Ohio State University, Columbus, OH, USA. Figure 4(a) shows the trajectories of the 9 satellites from the 5 LEO constellations. Figure 4(b) shows the initial and final position estimates. Figure 4(c) shows the true and estimated receiver's position. The final 3D position error was found to be 5.8 m, while the 2D position error was 5.1 m (i.e., upon considering only the east and north coordinates in the ENU frame). It is worth noting that the addition of the NOAA satellite Doppler measurements did not reduce the positioning error by much (reduction on the order of centimeters), compared to using 4 Starlink, 2 OneWeb, 1 Orbcomm, 1 Iridium NEXT LEO satellites (as presented in (Kozhaya et al., 2023)). This is due to the already favorable geometry of the four constellations.

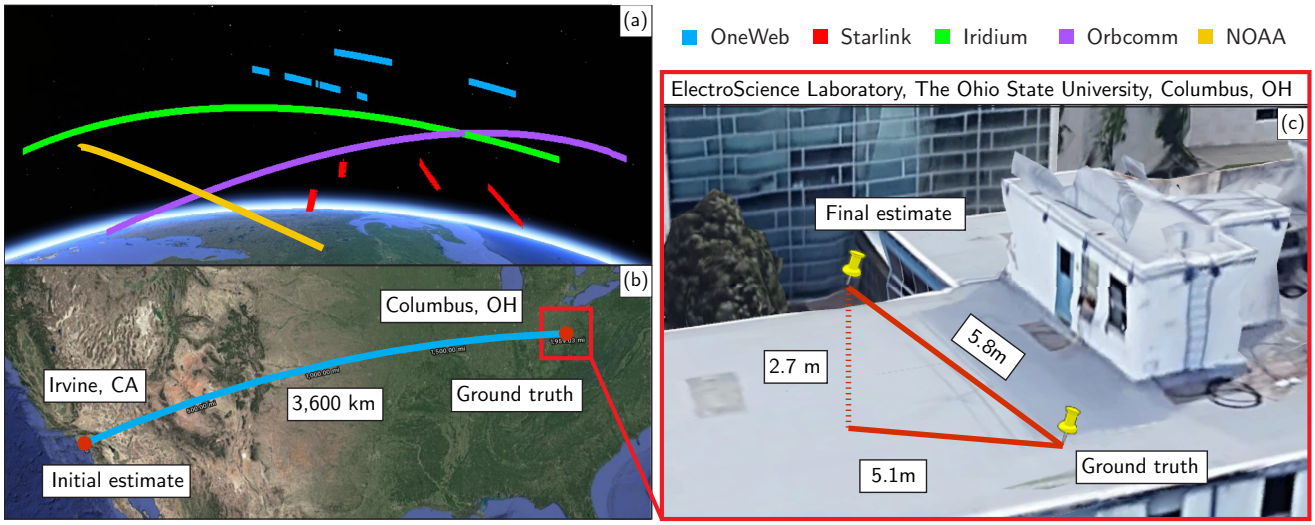

Figure 4: Positioning results with 4 Starlink, 2 OneWeb, 1 Orbcomm, 1 Iridium NEXT, and 1 NOAA LEO satellites: (a) LEO satellite trajectories. (b) Initial and final estimated positions. (c) Final errors relative to the receiver's true position.

VI. CONCLUSION

This paper showcased that the previously developed LEO-agnostic spectral-based approach is capable of acquiring and tracking a new LEO constellation: NOAA LEO satellites. Experimental results were also presented showing Hz-level Doppler tracking of 5 different LEO satellite constellations: Starlink, OneWeb, Orbcomm, Iridium NEXT, and NOAA. Carrier phase observables were constructed from the tracked Doppler and fused through an NLS estimator to localize a stationary receiver. Starting with an initial estimate 3,600 km away from the receiver's true position, the proposed approach achieved a 2D error of 5.1 m.

ACKNOWLEDGMENTS

This work was supported in part by the Office of Naval Research (ONR) under Grants N00014-19-1-2511 and N00014-22-1-2242, in part by the Air Force Office of Scientific Research (AFOSR) under Grant FA9550-22-1-0476, and in part by the U.S. Department of Transportation (USDOT) under Grant 69A3552047138 for the CARMEN University Transportation Center (UTC).

REFERENCES

3GPP (2010). Evolved universal terrestrial radio access (E-UTRA); multiplexing and channel coding. TS 36.212, 3rd Generation Partnership Project (3GPP).

3GPP (2018). Physical channels and modulation. TS 38.211, 5G; NR; 3rd Generation Partnership Project (3GPP).

3GPP2 (2011). Physical layer standard for cdma2000 spread spectrum systems (C.S0002-E). TS C.S0002-E, 3rd Generation Partnership Project 2 (3GPP2).

Bilardi, S. (2021). A GNSS signal simulator and processor for evaluating acquisition and tracking of GPS-like signals from

satellites in LEO. Master's thesis, University of Colorado at Boulder, CO, USA.

Bolcskei, H. (2001). Blind estimation of symbol timing and carrier frequency offset in wireless OFDM systems. *IEEE Transactions on Communications*, 49(6):988–999.

Burel, G. and Bouder, C. (2000). Blind estimation of the pseudo-random sequence of a direct sequence spread spectrum signal. In *Proceedings of IEEE Military Communications Conference*, volume 2, pages 967–970.

Cassel, R., Scherer, D., Wilburne, D., Hirschauer, J., and Burke, J. (2022). Impact of improved oscillator stability on LEO-based satellite navigation. In *Proceedings of ION International Technical Meeting*, pages 893–905.

Choi, H. and Moon, H. (2020). Blind estimation of spreading sequence and data bits in direct-sequence spread spectrum communication systems. *IEEE Access*, 8:148066–148074.

Curzi, G., Modenini, D., and Tortora, P. (2020). Large constellations of small satellites: A survey of near future challenges and missions. *Aerospace*, 7(9):1–18.

Egea-Roca, D., Lopez-Salcedo, J., Seco-Granados, G., and Falletti, E. (2022). Performance analysis of a multi-slope chirp spread spectrum signal for PNT in a LEO constellation. In *Proceedings of Workshop on Satellite Navigation Technology*, pages 1–9.

Farhangian, F., Benzerrouk, H., and Landry, R. (2021). Opportunistic in-flight INS alignment using LEO satellites and a rotatory IMU platform. *Aerospace*, 8(10):280–281.

Farhangian, F. and Landry, R. (2023). High-order pseudorange rate measurement model for multi-constellation LEO/INS integration: Case of Iridium-NEXT, Orbcomm, and Globalstar. *Proceedings of the Institution of Mechanical Engineers, Part G: Journal of Aerospace Engineering*, 237(4):925–939.

Flores, A. (2022). NAVSTAR GPS space segment/navigation user interfaces. `https://www.gps.gov/technical/icwg/IS-GPS-200N.pdf`.

Guo, F., Yang, Y., Ma, F., Liu, Y. Z. H., and Zhang, X. (2023). Instantaneous velocity determination and positioning using doppler shift from a LEO constellation. *Satellite Navigation*, 4:9–21.

Hartnett, M. (2022). Performance assessment of navigation using carrier Doppler measurements from multiple LEO constellations. Master's thesis, Air Force Institute of Technology, Ohio, USA.

Hendrickson, R. (1997). Globalstar for the military. In *Proceedings of IEEE Military Communications Conference*, volume 3, pages 1173–1178.

Huang, C., Qin, H., Zhao, C., and Liang, H. (2022). Phase - time method: Accurate Doppler measurement for Iridium NEXT signals. *IEEE Transactions on Aerospace and Electronic Systems*, 58(6):5954–5962.

Humphreys, T., Iannucci, P., Komodromos, Z., and Graff, A. (2023). Signal structure of the Starlink Ku-band downlink. *IEEE Transactions on Aerospace and Electronics Systems*. accepted.

Janssen, T., Koppert, A., Berkvens, R., and Weyn, M. (2023). A survey on IoT positioning leveraging LPWAN, GNSS and LEO-PNT. *IEEE Internet of Things Journal*, 10(13):11135–11159.

Jardak, N. and Jault, Q. (2022). The potential of LEO satellite-based opportunistic navigation for high dynamic applications. *Sensors*, 22(7):2541–2565.

Jiang, M., Qin, H., Su, Y., Li, F., and Mao, J. (2023). A design of differential-low Earth orbit opportunistically enhanced GNSS (D-LoeGNSS) navigation framework. *Remote Sensing*, 15(8):2136–2158.

Jiang, M., Qin, H., Zhao, C., and Sun, G. (2022). LEO Doppler-aided GNSS position estimation. *GPS Solutions*, 26(1):1–18.

Kanamori, H., Kobayashi, K., and Kubo, N. (2023). A map-matching based positioning method using Doppler tracking and estimation by a software-defined receiver for multi-constellation LEO satellites. In *Proceedings of ION International Technical Meeting*, pages 649–663.

Kassas, Z. (2021). Position, navigation, and timing technologies in the 21st century. volume 2, chapter 43: Navigation from low Earth orbit – Part 2: models, implementation, and performance, pages 1381–1412. Wiley-IEEE.

Kassas, Z., Khairallah, N., and Kozhaya, S. (2023a). Ad astra: Simultaneous tracking and navigation with megaconstellation LEO satellites. *IEEE Aerospace and Electronic Systems Magazine*. accepted.

Kassas, Z., Kozhaya, S., Saroufim, J., Kanj, H., and Hayek, S. (2023b). A look at the stars: Navigation with multi-constellation LEO satellite signals of opportunity. *Inside GNSS Magazine*, 18(4):38–47.

Kassas, Z., Morales, J., and Khalife, J. (2019). New-age satellite-based navigation – STAN: simultaneous tracking and navigation with LEO satellite signals. *Inside GNSS Magazine*, 14(4):56–65.

Kassas, Z., Neinavaie, M., Khalife, J., Khairallah, N., Haidar-Ahmad, J., Kozhaya, S., and Shadram, Z. (2021). Enter LEO on the GNSS stage: Navigation with Starlink satellites. *Inside GNSS Magazine*, 16(6):42–51.

Khairallah, N. and Kassas, Z. (2021). Ephemeris closed-loop tracking of LEO satellites with pseudorange and Doppler measurements. In *Proceedings of ION GNSS Conference*, pages 2544–2555.

Khalife, J. and Kassas, Z. (2023). Performance-driven design of carrier phase differential navigation frameworks with mega-constellation LEO satellites. *IEEE Transactions on Aerospace and Electronic Systems*, 59(3):2947–2966.

Khalife, J., Neinavaie, M., and Kassas, Z. (2022). The first carrier phase tracking and positioning results with Starlink LEO satellite signals. *IEEE Transactions on Aerospace and Electronic Systems*, 56(2):1487–1491.

Kozhaya, S., Kanj, H., and Kassas, Z. (2023). Multi-constellation blind beacon estimation, Doppler tracking, and opportunistic positioning with OneWeb, Starlink, Iridium NEXT, and Orbcomm LEO satellites. In *Proceedings of IEEE/ION Position, Location, and Navigation Symposium*, pages 1184–1195.

Kozhaya, S. and Kassas, Z. (2022). Blind receiver for LEO beacon estimation with application to UAV carrier phase differential navigation. In *Proceedings of ION GNSS Conference*, pages 2385–2397.

Kozhaya, S. and Kassas, Z. (2023). Positioning with Starlink LEO satellites: A blind Doppler spectral approach. In *Proceedings of IEEE Vehicular Technology Conference*, pages 1–5.

Li, L., Zhang, H., Du, S., Liang, T., and Gao, L. (2023). Blind despreading and deconvolution of asynchronous multiuser direct sequence spread spectrum signals under multipath channels. *IET Signal Processing*, 17(5):1–14.

Liu, S., Gao, Z., Wu, Y., Kwan Ng, D., Gao, X., Wong, K., Chatzinotas, S., and Ottersten, B. (2021). LEO satellite constellations for 5G and beyond: How will they reshape vertical domains? *IEEE Communications Magazine*, 59(7):30–36.

Liu, W., Wang, J., and Li, S. (2010). Blind detection and estimation of OFDM signals in cognitive radio contexts. In *Proceedings of International Conference on Signal Processing Systems*, volume 2, pages 347–351.

Menzione, F. and Paonni, M. (2023). LEO-PNT mega-constellations: a new design driver for the next generation MEO GNSS space service volume and spaceborne receivers. In *Proceedings of IEEE/ION Position, Location, and Navigation Symposium*, pages 1196–1207.

Merwe, J., Bartl, S., O'Driscoll, C., Rügamer, A., Förster, F., Berglez, P., Popugaev, A., and Felber, W. (2020). GNSS sequence extraction and reuse for navigation. In *Proceedings of ION GNSS+ Conference*, pages 2731–2747.

More, H., Cianca, E., and Sanctis, M. (2022). Positioning performance of LEO mega constellations in deep urban canyon environments. In *Proceedings of International Symposium on Wireless Personal Multimedia Communications*, pages 256–260.

Mortlock, T. and Kassas, Z. (2021). Assessing machine learning for LEO satellite orbit determination in simultaneous tracking and navigation. In *Proceedings of IEEE Aerospace Conference*, pages 1–8.

Morton, Y., Xu, D., and Jiao, Y. (2022). Ionospheric scintillation effects on signals transmitted from LEO satellites. In *Proceedings of ION GNSS Conference*, pages 2980–2988.

Neinavaie, M. and Kassas, Z. (2023). Unveiling Starlink LEO satellite OFDM-like signal structure enabling precise positioning. *IEEE Transactions on Aerospace and Electronic Systems*. accepted.

Neinavaie, M., Khalife, J., and Kassas, Z. (2021). Blind Doppler tracking and beacon detection for opportunistic navigation with LEO satellite signals. In *Proceedings of IEEE Aerospace Conference*, pages 1–8.

Neinavaie, M., Khalife, J., and Kassas, Z. (2022a). Acquisition, Doppler tracking, and positioning with Starlink LEO satellites: First results. *IEEE Transactions on Aerospace and Electronic Systems*, 58(3):2606–2610.

Neinavaie, M., Shadram, Z., Kozhaya, S., and Kassas, Z. M. (2022b). First results of differential Doppler positioning with unknown Starlink satellite signals. In *Proceedings of IEEE Aerospace Conference*, pages 1–14.

Orabi, M., Khalife, J., and Kassas, Z. (2021). Opportunistic navigation with Doppler measurements from Iridium Next and Orbcomm LEO satellites. In *Proceedings of IEEE Aerospace Conference*, pages 1–9.

Pinell, C., Prol, F., Bhuiyan, M., and Praks, J. (2023). Receiver architectures for positioning with low earth orbit satellite signals: a survey. *EURASIP Journal on Advances in Signal Processing*, 2023:60–80.

Prol, F., Ferre, R., Saleem, Z., Välisuo, P., Pinell, C., Lohan, E., Elsanhoury, M., Elmusrati, M., Islam, S., Celikbilek, K., Selvan, K., Yliaho, J., Rutledge, K., Ojala, A., Ferranti, L., Praks, J., Bhuiyan, M., Kaasalainen, S., and Kuusniemi, H. (2022). Position, navigation, and timing (PNT) through low earth orbit (LEO) satellites: A survey on current status, challenges, and opportunities. *IEEE Access*, 10:83971–84002.

Prol, F., Kaasalainen, S., Lohan, E., Bhuiyan, M., Praks, J., and Kuusniemi, H. (2023). Simulations using LEO-PNT systems: A brief survey. In *Proceedings of IEEE/ION Position, Location, and Navigation Symposium*, pages 1381–387.

Psiaki, M. (2021). Navigation using carrier Doppler shift from a LEO constellation: TRANSIT on steroids. *NAVIGATION, Journal of the Institute of Navigation*, 68(3):621–641.

Reid, T., Walter, T., Enge, P., Lawrence, D., Cobb, H., Gutt, G., O'Conner, M., and Whelan, D. (2021). Position, navigation, and timing technologies in the 21st century. volume 2, chapter 43: Navigation from low Earth orbit – Part 1: concept, current capability, and future promise, pages 1359–1379. Wiley-IEEE.

Ries, L., Limon, M., Grec, F., Anghileri, M., Prieto-Cerdeira, R., Abel, F., Miguez, J., Perello-Gisbert, J., d'Addio, S., R. Ioannidis and, A. O., Rapisarda, M., Sarnadas, R., and Testani, P. (2023). LEO-PNT for augmenting Europe's space-based PNT capabilities. In *Proceedings of IEEE/ION Position, Location, and Navigation Symposium*, pages 329–337.

Rui, Z., Ouyang, X., Zeng, F., and Xu, X. (2022). Blind estimation of GPS M-Code signals under noncooperative conditions. *Wireless Communications and Mobile Computing*, 2022.

Sabbagh, R. and Kassas, Z. (2023). Observability analysis of receiver localization via pseudorange measurements from a single LEO satellite. *IEEE Control Systems Letters*, 7(3):571–576.

Saroufim, J., Hayek, S., and Kassas, Z. (2023). Simultaneous LEO satellite tracking and differential LEO-aided IMU navigation. In *Proceedings of IEEE/ION Position Location and Navigation Symposium*, pages 179–188.

Shi, C., Zhang, Y., and Li, Z. (2023). Revisiting Doppler positioning performance with LEO satellites. *GPS Solutions*, 27(3):126–137.

Singh, U., Shankar, M., and Ottersten, B. (2022). Opportunistic localization using LEO signals. In *Proceedings of Asilomar Conference on Signals, Systems, and Computers*, pages 894–899.

Tan, Z., Qin, H., Cong, L., and Zhao, C. (2019). Positioning using IRIDIUM satellite signals of opportunity in weak signal environment. *Electronics*, 9(1):37.

Tanda, M. (2004). Blind symbol-timing and frequency-offset estimation in OFDM systems with real data symbols. *IEEE Transactions on Communications*, 52(10):1609–1612.

Tsatsanis, M. and Giannakis, G. (1997). Blind estimation of direct sequence spread spectrum signals in multipath. *IEEE Transactions on Signal Processing*, 45(5):1241–1252.

Wang, D., Qin, H., and Huang, Z. (2023). Doppler positioning of LEO satellites based on orbit error compensation and weighting. *IEEE Transactions on Instrumentation and Measurement*, 72:1–11.

Wei, Q., Chen, X., and Zhan, Y. (2020). Exploring implicit pilots for precise estimation of LEO satellite downlink Doppler frequency. *IEEE Communications Letters*, 24(10):2270–2274.

Wu, N., Qin, H., and Zhao, C. (2023). Long-baseline differential doppler positioning using space-based SOP based on BPVGMM. *IEEE Transactions on Instrumentation and Measurement*, 72:1–10.

Yang, C. and Soloviev, A. (2023). Starlink Doppler and Doppler rate estimation via coherent combining of multiple tones for opportunistic positioning. In *Proceedings of IEEE/ION Position, Location, and Navigation Symposium*, pages 1143–1153.

Yang, C., Zang, B., Gu, B., Zhang, L., Dai, C., Long, L., Zhang, Z., Ding, L., and Ji, H. (2023). Doppler positioning of dynamic targets with unknown LEO satellite signals. *Electronics*, 12(11):2392–2404.

Ye, L., Gao, N., Yang, Y., Deng, L., and Li, H. (2023). Three satellites dynamic switching range integrated navigation and positioning algorithm with clock bias cancellation and altimeter assistance. *Aerospace*, 10(5):411–438.

Zhao, C., Qin, H., Wu, N., and Wang, D. (2023). Analysis of baseline impact on differential doppler positioning and performance improvement method for LEO opportunistic navigation. *IEEE Transactions on Instrumentation and Measurement*, 72:1–10.